Int. J. Electrochem. Sci., 7 **(2012)** 9161 - 9173

International Journal of
ELECTROCHEMICAL
SCIENCE
www.electrochemsci.org

Poly(brilliant cresyl blue) Electrodeposited on Multi-Walled Carbon Nanotubes Modified Electrode and Its Application for Persulfate Determination

Kuo-Chiang Lin, Jia-Yan Huang, Shen-Ming Chen[*]

Electroanalysis and Bioelectrochemistry Lab, Department of Chemical Engineering and Biotechnology, National Taipei University of Technology, No.1, Section 3, Chung-Hsiao East Road, Taipei 106, Taiwan (ROC).
[*]E-mail: smchen78@ms15.hinet.net

Received: 31 July 2012 / *Accepted:* 6 September 2012 / *Published:* 1 October 2012

Poly(brilliant cresyl blue) (PBCB) has been successfully electrodeposited on multi-walled carbon nanotubes (MWCNT) to form PBCB-MWCNT modified electrode by repeatedly cyclic voltammetry. MWCNT enables the higher current response in the hybrid composite when compared to the PBCB formation without using MWCNT. Well redox peak current development in the film formation indicates that MWCNT provides more electroactive surface areas for PBCB deposition and reduces the disorder situation of polymer chains. It is stable in various scan rates and different pH conditions. The surface coverage of BCB and PBCB was estimated in 7.4×10^{-11} and 7.6×10^{-11} mol cm^{-2} at PBCB-MWCNT/GCE higher than that at PBCB/GCE. More deposition amount indicates that MWCNT can provide more space for both BCB and PBCB. It shows lower over-potential and higher current response to persulfate when compared to the bare and PBCB electrodes. More obvious reduction currents are found using LSV technique. Applied potential at -0.03 V, it shows the sensitivity of 124.5 and 21.2 μA mM^{-1} cm^{-2} for the linear concentration range of 10^{-5}–10^{-4} and 3.1×10^{-3}–1.01×10^{-1} M, and detection limit of 1 μM (S/N = 3).

Keywords: Brilliant cresyl blue (BCB), Multi-walled carbon nanotubes (MWCNT), Persulfate, Electropolymerization, Electrochemistry, Electrocatalysis, Chemical sensors

1. INTRODUCTION

Due to a gradual increase in the use of persulfate for remediation of contaminated soil and groundwater, a simple and convenient measurement of persulfate concentration at the field site is desired to evaluate its efficiency at designated time intervals at the on/off site. Several methods have been reported in the literature for the quantitative determination of persulfate. These methods include

reductometric [1,2], polarographic [3–5], and spectrophotometric [6,7] methods. Although some of these methods use automated flow injection system with either colorimetric or electrochemical detection, it is not feasible for the routine analysis of vast number samples. In addition, Huang et al. [7] developed a spectrophotometric method by mixing sulfuric acid and ferrous ammonium sulfate with a sample containing persulfate and allowing to react for 40 min before adding ammonium thiocyanate. However, the requirement of a long equilibrium period is a disadvantage of this method. In order to overcome this problem, Liang et al. reported a rapid spectrophotometric determination of persulfate anion using *in situ* chemical oxidation (ISCO) [8].

Among these methods, electrochemical method [9–14] is valuable to use for the further study due to simple operation, fast response, and low cost, except of other advantages. The modification of electrode surfaces with inorganic or organic coatings often avoids some drawbacks and represents a rapid and versatile resource for the preparation of stable and selective new electrochemical sensors [15-24]. The determination of persulfate (peroxodisulphate) by direct current voltammetry using carbon paste electrodes with incorporated Prussian blue (PB), the objective was to investigate the electroanalytical utility of PB films on platinum electrodes to the determination of persulfate [25]. A flow-injection system with a PB film modified electrode is proposed for the determination of persulfate by amperometry [26]. Recent researches have also been noticed on the electropolymerization of some aromatic compounds on a GCE surface, e.g. some authors devoted in electrochemical glutathione sensor based on electrochemically deposited poly-m-aminophenol [27].

Since the discovery of carbon nanotubes (CNTs) by lijima in 1991 [28], research on CNTs have improved speedily and have become one of the most attractive parts of nanotechnology in the world [29,30]. These nanotubes are known to possess interesting chemical and physical properties such as electric conductivity, chemical stability, mechanical and tensile strength [31,32]. In the electrochemical sensors, the good electrocatalytic activities of CNTs are also attractive. Therefore, more and more sensors relative to CNTs hybrid composites with organic or inorganic compounds are reported [33,34].

In azine dyes brilliant cresyl blue (BCB) is a cationic quinine-imide dye with a planar rigid structure with promising properties as a redox catalyst with features like fast rate of charge transfer and ion transport [35–37]. Previous studies reported poly(brilliant cresyl blue) (PBCB) can be synthesized by electrochemical polymerization of BCB. These studies reported also the growth mechanism of PBCB along with the electrochemical studies [36,37]. In our previous work, we ever prepared multi-walled carbon nanotubes (MWCNT) and PBCB on the electrode surface to form a composite film (PBCB-MWCNT) [38]. It was characterized and understood by its electrocatalytic activity along with its application in the determination of folic acid. This good electrocatalytic activity provides a chance to do the further investigation for the determination of persulfate.

In this work, the PBCB film was prepared on bare electrode or MWCNT-modified electrode by the electropolymerization of BCB monomers. The PBCB film formation on MWCNT-modified electrode was compared and expected to have more well deposition due to more electroactive surface areas contributed by MWCNT to avoid the disorder of polymer chains in the deposition process. It was examined in different scan rate and pH conditions to characterize this electroactive composite in the electrode interface, electrochemical process, and stability. The electrocatalytic reduction of persulfate

was compared with bare and PBCB modified electrodes to study the over-potential and the current response to persulfate. This electroactive species modified electrode can be used as an amperometric sensor to determine persulfate.

2. MATERIALS AND METHODS

2.1. Reagents

Brilliant cresyl blue (BCB), multi-walled carbon nanotubes (MWCNT), and persulfate (peroxodisulphate) were purchased from Sigma-Aldrich (USA). All other chemicals (Merck) used were of analytical grade (99%). Double distilled deionized water was used to prepare all the solutions. A phosphate buffer solution (PBS) of pH 7 was prepared using Na_2HPO_4 (0.05 M) and NaH_2PO_4 (0.05 M).

2.2. Apparatus

All electrochemical experiments were performed using CHI 1205a potentiostats (CH Instruments, USA). The working electrode was glassy carbon electrode (GCE) using BAS GCE (with diameter of 0.3 cm, geometric surface area of 0.07 cm^2, Bioanalytical Systems, Inc., USA). Electrochemical experiments carried out with a conventional three-electrode system which consisted of an Ag/AgCl (3M KCl) as a reference electrode, a GCE as a working electrode, and a platinum wire as a counter electrode. The buffer solution was entirely altered by deaerating with nitrogen gas atmosphere. The electrochemical cells were kept properly sealed to avoid the oxygen interference from the atmosphere. Prior to modification, the GCE was mechanically polished with BAS polishing kit (Bioanalytical Systems, Inc., USA) and alumina powder (0.05 μm) to mirror finish and ultrasonicated in double distilled water for 3 min. Prior to the electrochemical experiments, the buffer solution was deoxygenated with nitrogen for 10 min.

2.3. Preparation of PBCB and PBCB-MWCNT film modified electrodes

The PBCB modified electrode was prepared by the electropolymerization of BCB monomers in neutral solution using bare GCE electrode. The electro-active system was electro-generated in situ from BCB oxidation, the electrode applied in the potential range of -0.6–1.0 V (vs. Ag/AgCl) with scan rate of 100 mV s^{-1} and 20 scan cycles in 0.1 M PBS (pH 7) containing 1×10^{-4} M BCB monomers. The prepared electrode, PBCB/GCE, was stored in the refrigerator at 4 ℃ for further study in this work.

The PBCB-MWCNT modified electrode was prepared by the electropolymerization of BCB monomers in neutral solution using MWCNT-modified GCE (MWCNT/GCE). Prior to the electropolymerization of BCB the GCE was firstly coated with MWCNT which was functionalized with carboxylic group by acidic treatment. The electro-active system was electro-generated in situ from BCB oxidation, the MWCNT/GCE electrode applied in the potential range of -0.6–1.0 V (vs.

Ag/AgCl) with scan rate of 100 mV s^{-1} and 20 scan cycles in 0.1 M PBS (pH 7) containing 10^{-4} M BCB monomers. The prepared electrode, PBCB-MWCNT/GCE, was stored in the refrigerator at 4 ℃ for further study in this work.

3. RESULTS AND DISCUSSION

3.1. Electrochemical formation of PBCB film on GCE and MWCNT/GCE

The PBCB film formation involving the electropolymerization of BCB monomers was investigated by cyclic voltammetry using GCE and MWCNT/GCE, respectively.

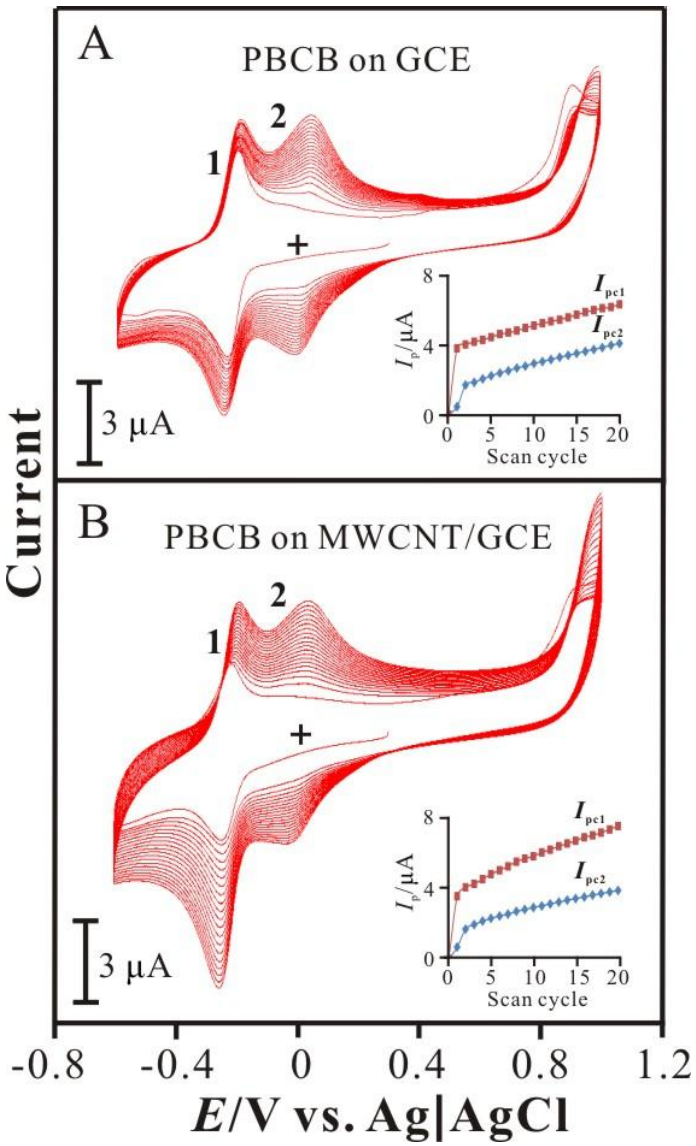

Figure 1. Cyclic voltammograms of PBCB form on (A) bare GCE and (B) MWCNT/GCE in pH 7 PBS containing 1×10^{-4} M BCB. Scan rate = 0.1 Vs^{-1}. Insets: the plots of the cathodic peak currents (I_{pc1} & I_{pc2}) vs. scan cycles.

Fig. 1 displays the consecutive cyclic voltammograms of BCB electropolymerzation in pH 7 PBS using (A) GCE and (B) MWCNT/GCE, respectively. Only one cathodic peak was found at E_{pc1} = -246 mV in the first scan segment when the initial potential was started from +0.3 V. It is recognized as the reduction peak of BCB monomer redox processes. Hereafter, another cathodic peak appeared at E_{pc2} = -65 mV in the third scan segment after scanning to more positive potential at +1.0 V. This is due to the sufficient positive potential to initiate BCB monomers to BCB radical results in the electropolymerization. Therefore, the voltammograms were characterized by two well-defined redox couples, with the formal potential occurring at $E^{0'}{}_1$ = -217 mV, $E^{0'}{}_2$ = 20 mV; and $E^{0'}{}_1$ = -221 mV, $E^{0'}{}_2$ = 13 mV (vs. Ag/AgCl) at GCE and MWCNT/GCE, respectively. The redox couple 1 & 2 is attributed to the reduced and oxidized forms of BCB monomer and PBCB polymer [37-39], respectively. No too much peak shifting in the PBCB electro-deposition at GCE and MWCNT/GCE results in almost the same redox processes in the voltammograms. However, the peak currents are higher at MWCNT/GCE due to the more active surface areas contributed by MWCNT. It also indicates that the PBCB film formed on MWCNT/GCE very well. Insets show the correlation between cathodic peak currents (I_{pc1} & I_{pc2}) and scan cycle, the current is increasing as the increase of scan cycle on both GCE and MWCNT/GCE. Particularly, the cathodic peak 2 is found much higher at MWCNT/GCE than GCE. This might indicate that the MWCNT enhance the cathodic peak current for BCB monomer.

3.2. Electrochemical characteristics of PBCB-MWCNT composites

The PBCB and PBCB-MWCNT composites were individually examined with various scan rates by cyclic voltammetry.

Fig. 2 shows the cyclic voltammograms of the PBCB-MWCNT/GCE examined with scan rate of 10–500 mV s^{-1} in pH 7 PBS. The formal potential of the redox couples is found similar to those in the preparation procedure as shown in Fig. 1. Both anodic and cathodic peak currents are also directly proportional to scan rate up to 500 mV s^{-1} (insets of Fig. 2) as expected for surface confined process. This also means that this process is diffusion-less controlled and stable in the electrochemical system. The observation of well-defined and the persistent cyclic voltammetric peaks indicate that both PBCB/GCE and PBCB-MWCNT/GCE exhibit electrochemical response characteristics of redox species confined on the electrode surface.

This film modified electrodes show the linear regressing equation of peak currents (I_{pa} & I_{pc}) and scan rate (v) can be expressed as follows:

At PBCB/GCE:

$$I_{pc1}(\mu A) = 0.015v(\text{mV s}^{-1}) + 0.64 \ (R^2 = 0.996) \quad (1)$$

$$I_{pa1}(\mu A) = -0.004v(\text{mV s}^{-1}) - 0.32 \ (R^2 = 0.991) \quad (2)$$

$$I_{pc2}(\mu A) = 0.016v(\text{mV s}^{-1}) + 0.51 \ (R^2 = 0.996) \quad (3)$$

$$I_{pa2}(\mu A) = -0.017v(\text{mV s}^{-1}) - 0.79 \ (R^2 = 0.988) \quad (4)$$

At PBCB-MWCNT/GCE:

$$I_{pc1}(\mu A) = 0.029v(\text{mV s}^{-1}) + 1.35 \ (R^2 = 0.996) \quad (5)$$

$$I_{pa1}(\mu A) = -0.01v(\text{mV s}^{-1}) - 0.96 \ (R^2 = 0.972) \quad (6)$$

$$I_{pc2}(\mu A) = 0.018v(\text{mV s}^{-1}) + 0.51 \ (R^2 = 0.996) \quad (7)$$

$$I_{pa2}(\mu A) = -0.023v(\text{mV s}^{-1}) - 0.84 \ (R^2 = 0.996) \quad (8)$$

Moreover, the ratio of oxidation-to-reduction peak currents is nearly unity in redox couple 2 and formal potentials do not change with increasing scan rate in this pH condition. This result reveals that the electron transfer kinetics is very fast on the electrode modified surface.

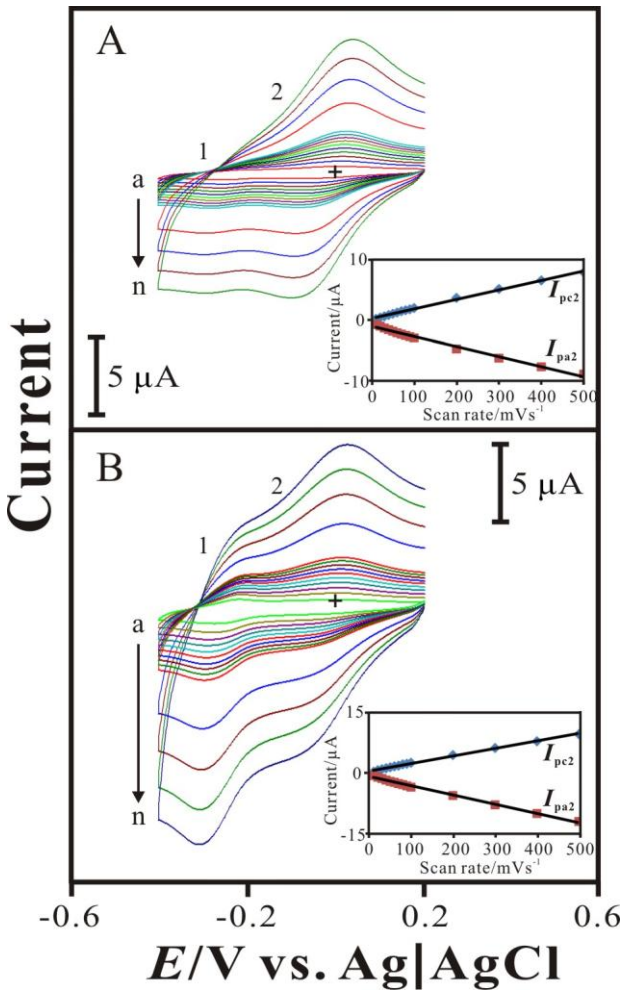

Figure 2. Cyclic voltammograms of (A) PBCB/GCE and (B) PBCB-MWCNT/GCE examined in pH 7 PBS with various scan rates from 10 to 500 mVs^{-1} (a ➔ n). Insets: the plots of the peak currents (I_{pa} & I_{pc}) vs. scan rate.

We have estimated, the apparent surface coverage (Γ), by using Eq. (9) [40]:

$$I_p = n^2F^2vA\Gamma/4RT \quad (9)$$

where, I_p is the peak current of the PBCB or PBCB-MWCNT composite electrode; n is the number of electron transfer; F is Faraday constant (96485 C/mol); v is the scan rate (V s^{-1}); A is the area of the electrode surface (0.07 cm^2); R is gas constant (8.314 J mol^{-1} K^{-1}); and T is the room temperature (298.15 K). In the present case as shown in Table 1, the calculated surface coverage (Γ) was $\Gamma_{BCB} = 3.8\times10^{-11}$ mol cm^{-2} and $\Gamma_{PBCB} = 6.1\times10^{-11}$ mol cm^{-2} for assuming a one-electron process at PBCB/GCE. At PBCB-MWCNT/GCE, it was estimated as $\Gamma_{BCB} = 7.4\times10^{-11}$ mol cm^{-2} and $\Gamma_{PBCB} = 7.6\times10^{-11}$ mol cm^{-2}. This is known that more deposition amount of BCB and PBCB on MWCNT/GCE indicating that the MWCNT helps the deposition of electroactive species.

Table 1. Surface coverage of BCB and PBCB formed at PBCB/GCE and PBCB-MWCNT/GCE.

Surface coverage (Γ, mol cm^{-2})	Γ_{BCB} [a]	Γ_{PBCB} [b]
PBCB/GCE	3.8×10^{-11}	6.1×10^{-11}
PBCB-MWCNT/GCE	7.4×10^{-11}	7.6×10^{-11}

[a] Γ_{BCB}: the surface coverage estimated in redox couple 1.
[b] Γ_{PBCB}: the surface coverage estimated in redox couple 2.

Fig. 3A shows the voltammograms of bare GCE, PBCB/GCE, and PBCB-MWCNT/GCE examined in pH 7 PBS. Compared to bare electrode, the modified electrodes exhibit two obvious redox couples. As shown in Table 2, peak-to-peak separation is found with small value less than 90 mV. It indicates that the electron transfer is very fast at both PBCB/GCE and PBCB-MWCNT/GCE. This solution is one of the suitable conditions to these electroactive species. Particularly, higher current response is found at PBCB-MWCNT/GCE indicating that the PBCB-MWCNT is more electroactive to be the proposed material.

Table 2. Estimation of peak-to-peak separation (ΔE_p) at PBCB and PBCB-MWCNT modified electrodes.

Modified electrodes	ΔE_{p1} [a]/mV	ΔE_{p2} [b]/mV
PBCB/GCE	67	72
PBCB-MWCNT/GCE	86	54

[a] ΔE_{p1}: the peak-to-peak separation estimated in redox couple 1.
[b] ΔE_{p2}: the peak-to-peak separation estimated in redox couple 2.

Fig. 3B displays the pH-dependent voltammetric response of PBCB-MWCNT modified electrode. In order to ascertain this, the voltammetric responses of PBCB-MWCNT electrode were obtained in the solutions of different pH values varying from 1 to 13. The formal potential of the redox couples is pH-dependent with negative shifting as increasing pH value of the buffer solution. The inset in Fig. 3B shows the formal potential ($E^{0'}$) of the PBCB-MWCNT/GCE plotted over a pH range of 1—13. It shows a slope of $E^{0'}{}_1$ = -50 mV pH^{-1} and $E^{0'}{}_2$ = -51 mV pH^{-1}, which is close to that given by the Nernstian equation for equal number of electrons and protons transfer processes. The phenomenon

indicates that the number of electrons and protons might be the same. It exists in the form of reduced and oxidized segments, or as only oxidized dimeric segments. The above result shows that the PBCB-MWCNT film is stable and electrochemically active in the aqueous buffer solutions.

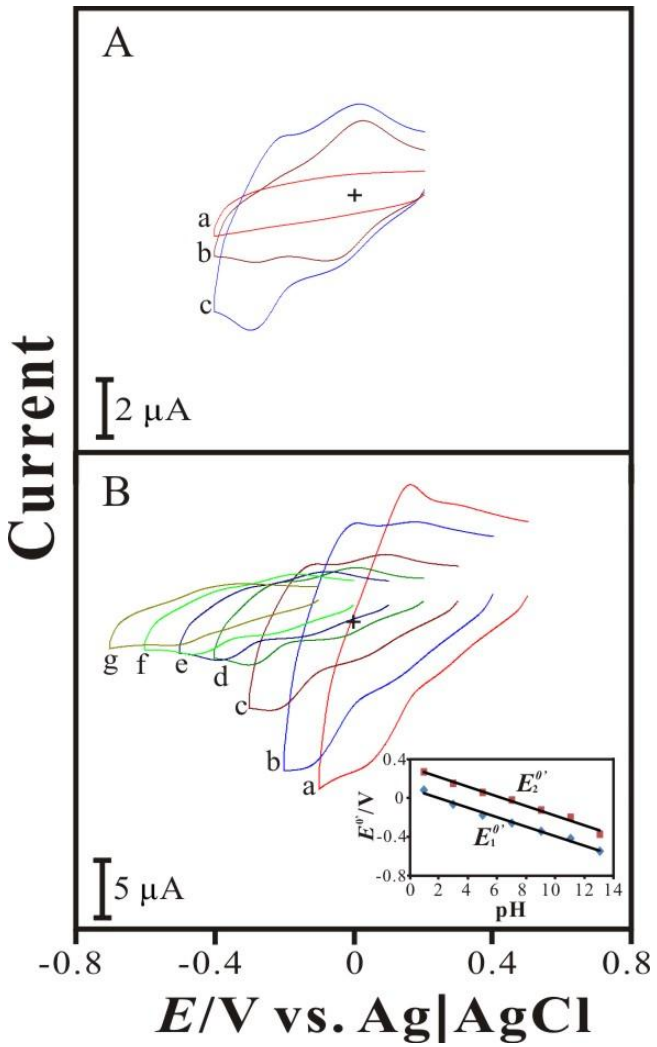

Figure 3. (A) Cyclic voltammograms of (a) bare GCE, (b) PBCB/GCE, and (c) PBCB-MWCNT/GCE examined in pH 7 PBS. (B) Cyclic voltammograms of PBCB-MWCNT/GCE examined with various pH conditions from pH 1 to 13 (a ➔ g). Scan rate = 0.1 Vs^{-1}. Inset: the plots of the formal potential ($E^{0'}$) vs. pH.

3.3. Electrocatalytic reduction of persulfate by PBCB and PBCB-MWCNT films

The electroactive species, PBCB and PBCB-MWCNT, were investigated for the electrocatalytic reduction of persulfate.

Fig. 4 shows the cyclic voltammograms of persulfate examined in pH 7 PBS using (A) PBCB/GCE and (B) PBCB-MWCNT/GCE, respectively. Both PBCB/GCE and PBCB-MWCNT/GCE exhibit electrocatalytic reduction peaks at about -0.03 V and -0.29 V. It can be found that the anodic peak current is increasing as the increase of persulfate concentration. Particularly, the PBCB-

MWCNT/GCE show the better electrocatalytic reduction current to persulfate as compared with bare electrode and PBCB/GCE in the insets of Fig. 4.

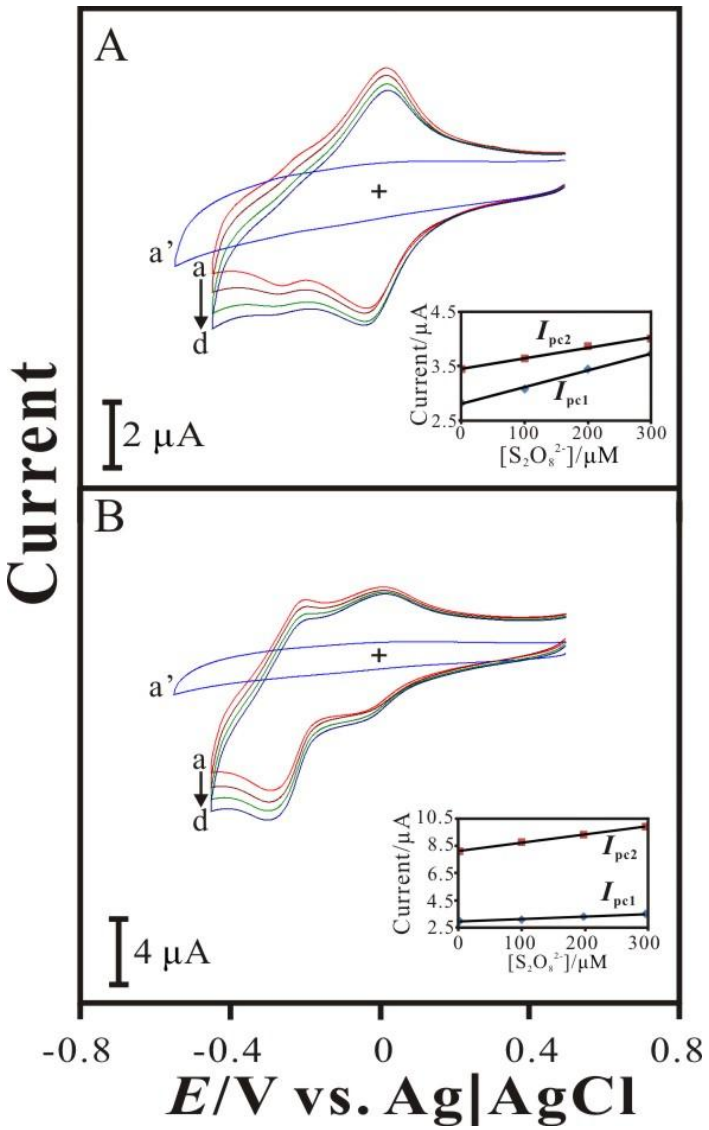

Figure 4. Cyclic voltammograms of (A) PBCB/GCE and (B) PBCB-MWCNT/GCE examined in pH 7 PBS containing $[S_2O_8^{2-}]$ = (a) 0, (b) 100, (c) 200, and (d) 300 μM, respectively. (a') is the bare GCE examined in the maximal $S_2O_8^{2-}$ concentration. Scan rate = 0.1 Vs^{-1}. Insets: the plots of the cathodic peak currents (I_{pc1} & I_{pc2}) vs. $[S_2O_8^{2-}]$.

Fig. 5 shows the linear sweep voltammograms (LSV) of persulfate using PBCB-MWCNT/GCE in pH 7 PBS. The PBCB-MWCNT/GCE exhibits electrocatalytic reduction peaks at about -0.03 V and -0.25 V for persulfate. It can be also found that the cathodic peak current is increasing as the increase of persulfate concentration. By above results, one can conclude that the PBCB-MWCNT has lower over-potential and higher current response to persulfate.

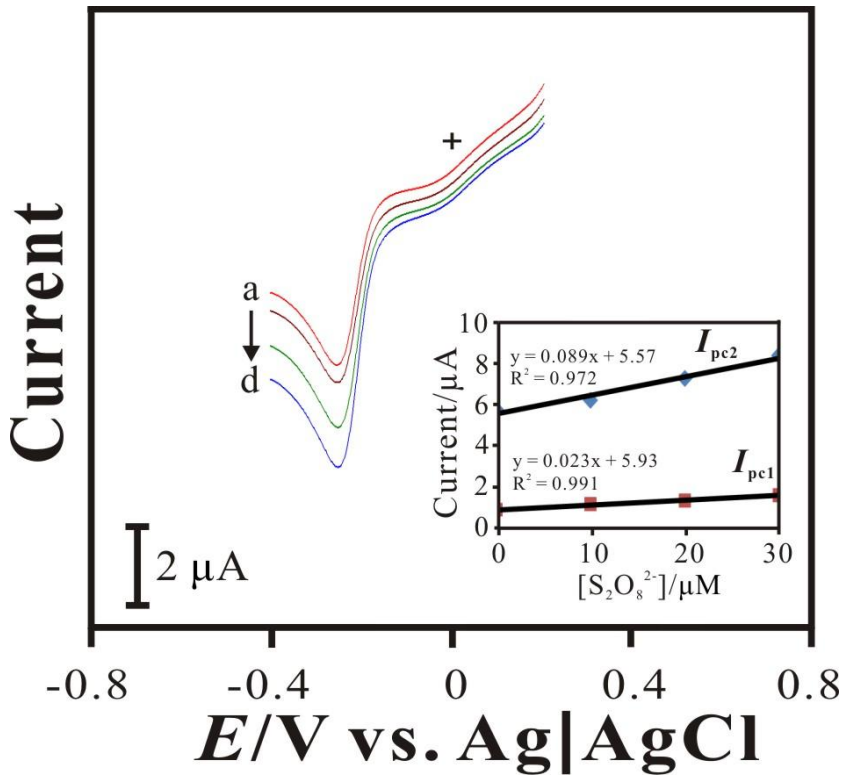

Figure 5. Linear sweep voltammograms of PBCB-MWCNT/GCE examined in pH 7 PBS containing $[S_2O_8^{2-}]$ = (a) 0, (b) 10, (c) 20, and (d) 30 μM, respectively. Insets: the plots of the cathodic peak currents (I_{pc1} & I_{pc2}) vs. $[S_2O_8^{2-}]$.

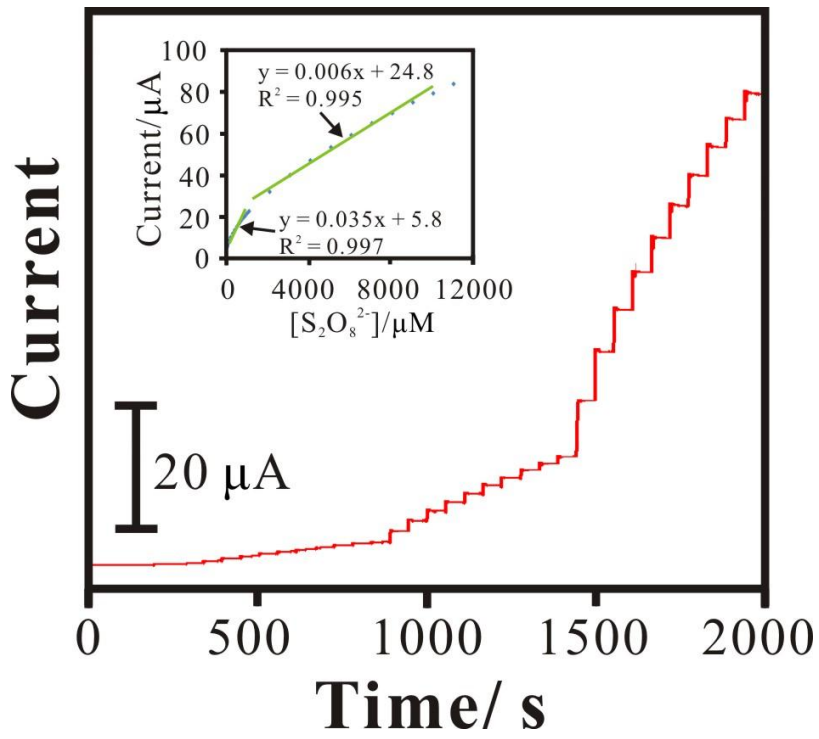

Figure 6. Amperograms of PBCB-MWCNT/GCE examined in pH 7 PBS with several additions of $[S_2O_8^{2-}]$ = 10-11100 μM, respectively. Electrode rotation speed = 1000 rpm. $E_{app.}$ = -0.03 V. Inset: the plot of the peak currents vs. $[S_2O_8^{2-}]$.

The PBCB-MWCNT electroactive species was further immobilized on rotating disk electrode to study the amperometric current response by amperometry.

Fig. 6 shows the amperograms of PBCB-MWCNT/GCE examined in pH 7 PBS with several additions of persulfate (10 μM per 50 seconds) when applied potential at -0.03 V and set electrode rotation speed at 1000 rpm.

This film modified electrode shows linear correlation between the electrocatalytic reduction currents (I_p) and species concentration (C_i), and the linear regressing equations can be expressed as follows:

$$I_p(\mu A) = 0.035C_i(\mu M) + 5.8 \ (R^2 = 0.997) \quad (10)$$

$$I_p(\mu A) = 0.006C_i(\mu M) + 24.8 \ (R^2 = 0.995) \quad (11)$$

It is calculated with the sensitivity of 124.5 and 21.2 μA mM^{-1} cm^{-2} for the linear concentration range of 10^{-5}-10^{-4} M and 3.1×10^{-3}-1.01×10^{-1} M, and detection limit of 1 μM (S/N = 3). The performance of this sensor can be known and compared with other methods as shown in Table 3. It's obviously competitive using our method by the comparison. Particularly, the limit of detection is so low and attractive in this literature.

Table 3. Performance of persulfate determination using different methods.

Methods	Working Point	LOD[a]/μM	LCR[b]/M	Sensitivity/μA mM^{-1} cm^{-2}	Reference
Voltammetry	0.2 V	41.9	5×10^{-5}–3×10^{-3}	9.356	[25]
Flow injection amperometry	0.025 V	90	1×10^{-4}–1×10^{-3}	144	[26]
Spectrophotometry	352 nm	50	0–0.07	0.118 Abs. mM^{-1}	[8]
Amperometry	-0.03 V	1	10^{-5}–10^{-4}; 3.1×10^{-3}–1.01×10^{-1}	124.5; 21.2	This Work

[a] LOD: limit of detection.
[b] LCR: linear concentration range.

By above results, one can conclude that the PBCB-MWCNT is a good electroactive species as catalyst to determine persulfate with lower over-potential and higher current response.

4. CONCLUSIONS

The PBCB-MWCNT composites have been successfully prepared on electrode surface by the electropolymerization of BCB on MWCNT-modified electrode. The film formation on MWCNT-

modified electrode is very well due to more electroactive surface areas to avoid the disorder of polymer chains. It is surface-confined and stable in various scan rate and different pH conditions. As compared with bare and PBCB modified electrodes, the PBCB-MWCNT modified electrode shows lower over-potential and higher current response to persulfate. This electroactive species modified electrode can be used as an amperometric persulfate sensor due to the advantages of simple operation, fast response, and low cost.

ACKNOWLEDGEMENTS
This work was supported by the National Science Council of Taiwan (ROC).

References

1. I.M. Kolthoff, V.A. Stenger, *Volumetric Analysis, second ed. Vol. I: Theoretical Fundamentals. Vol. II: Titration Methods: Acid–Base, Precipitation and Complex Reactions*. Interscience Publishers Inc., New York (1947).
2. I.M. Kolthoff, E.M. Carr, *Anal. Chem.* 25 (1953) 298–301.
3. I.M. Kolthoff, R.J. Woods, *J. Am. Chem. Soc.* 88 (1966) 1371–1375.
4. D. Amin, *Analyst* 106 (1981) 1217–1221.
5. D. Amin, A.K. Hareez, *Analyst* 106 (1981) 1221–1224.
6. P.M. Shuiundu,, A.P. Wade,, S.B. Jonnalagadda, *Can. J. Chem.* 68 (1990) 1750–1756.
7. K.C. Huang, R.A. Couttenye, G.E. Hoag, *Chemosphere* 49 (2002) 413–420.
8. C. Liang, C.F. Huang, N. Mohanty, R.M. Kurakalva, *Chemosphere* 73 (2008) 1540–1543.
9. P.A. Dimovasilis, M.I. Prodromidis, *Sens. Actuators B* 156 (2011) 689–694.
10. X. Xing, S. Liu, J. Yu, W. Lian, J. Huang, *Biosens. Bioelectron.* 31 (2012) 277–283.
11. S. Pakapongpan, R. Palangsuntikul, W. Surareungchai, *Electrochim. Acta* 56 (2011) 6831–6836.
12. J. Li, H. Xie, L. Chen, *Sens. Actuators B* 153 (2011) 239–245.
13. L. Yuan, J. Zhang, P. Zhou, J. Chen, R. Wang, T. Wen, Y. Li, X. Zhou, H. Jiang, *Biosens. Bioelectron.* 29 (2011) 29–33.
14. X. Li, Z. Chen, Y. Zhong, F. Yang, J. Pan, Y. Liang, *Anal. Chim. Acta* 710 (2012) 118–124.
15. B. Unnikrishnan, Y. Umasankar, S. M. Chen, C. C. Ti, *Int. J. Electrochem. Sci.* 7(2012) 3047-3058.
16. Y. Umasankar, B. Unnikrishnan, S. M. Chen, T. W. Ting, *Int. J. Electrochem. Sci.* 7(2012) 484-498.
17. S. M. Chen, C. H. Wang, K. C. Lin, Int. *J. Electrochem. Sci.* 7(2012) 405-425.
18. A. P. Periasamy, Y. H. Ho, and S. M. Chen, Biosensors and Bioelectronics, 29(2011) 151-158.
19. Y. Li, J. Y. Yang, S. M. Chen, *Int. J. Electrochem. Sci.* 6 (2011) 4829-4842.
20. Y. Li, S. Y. Yang, S. M. Chen, *Int. J. Electrochem. Sci.* 6 (2011) 3982-3996.
21. K. C. Lin, C. Y. Yin, S. M Chen, Int. J. Electrochem. Sci. 6 (2011) 3951-3965.
22. K. C. Lin, T. H. Tsai, S. M. Chen, *Biosensors and Bioelectronics*, 26(2010) 608-614.
23. S. Thiagarajan, T. H. Tsai, S. M. Chen, *Biosensors and Bioelectronics*, 24(2009) 2712-2715.
24. S. A. Kumar, P. H. Lo, S. M. Chen, *Biosensors and Bioelectronics*, 24(2008)518-523.
25. M.F.D. Oliveira, R.J. Mortimer, N.R. Stradiotto, *Microchem. J.* 64 (2000) 155-159.
26. M.F.D. Oliveira, A.A. Saczk, J.A.G. Neto, P.S. Roldan, N.R. Stradiotto, *Sensors* 3 (2003) 371-380.
27. Y. Oztekin, A. Ramanaviciene, A. Ramanavicius, *Electroanalysis* 23 (2011) 701–709.
28. S. Iijima, *Nature* 354 (1991) 56-58.
29. W. Yue-Rong, H. Ping, L. Qiong-Lin, L. Guo-An, W. Yi-Ming, *Chin. J. Anal. Chem.* 36(8) (2008)

1011-1016.
30. D.S. Bag, R. Dubey, N. Zhang, J. Xie, V.K. Varadan, D. Lal, G.N. Mathur, *Smart. Mater. Struct.* 13 (2004) 1263-1267.
31. M. Valcarcel, B.M. Simonet, S. Cardenas, B. Zuarez, *J. Anal. bioanal. Chem.* 382 (2005) 1783-1790.
32. A.S. Adekunle, B.O. Agloola, J. Pillay, K.I. Ozoemena, Sens. Actuartor. B 148 (2010) 93-112.
33. Y.L. Yang, B. Unnikrishnan, S.M. Chen, *Int. J. Electrochem. Sci.*, 6 (2011) 3902 – 3912.
34. A.M. Farah, N.D. Shooto, F.T. Thema, J.S. Modise, E.D. Dikio, *Int. J. Electrochem. Sci.*, 7 (2012) 4302 – 4313.
35. D.W. Yang, H.H. Liu, *Biosens. Bioelectron.* 25 (2009) 733-745.
36. A. Balamurugan, S.M. Chen, *J. Solid State Electrochem.* 14 (2010) 35-41.
37. M.E. Ghica, C.M.A. Brett, *J. Electroanal. Chem.* 629 (2009) 35-42.
38. Y. Umasankar, T.W. Ting, S.M. Chen, *J. Electrochem. Soc.* 158 (2011) K117-K122.
39. M. Chen, J.Q. Xu, S.N. Ding, D. Shan, H.G. Xue, S. Cosnier, M. Holzinger, *Sens. Actuators B* 152 (2011) 14–20.
40. E. Laviron, *J. Electroanal. Chem.* 52 (1974) 355–393.